Sub Topic: Laminar Flames

10th U. S. National Combustion Meeting
Organized by the Eastern States Section of the Combustion Institute
April 23-26, 2017
College Park, Maryland

Understanding Crystal Phase Equilibrium of TiO_2 in Flames

Changran Liu[1], Joaquin Camacho[2], Hai Wang[1,]*

[1]Mechanical Engineering Department, Stanford University, Stanford, CA 94305, USA
[2] Mechanical Engineering Department, San Diego State University, San Diego, CA 92189, USA
[*]Corresponding Author Email: haiwang@stanford.edu

Abstract: Nano-scale titanium oxide (TiO_2) is a useful material for a wide range of applications. In a previous study, we showed that the crystal phase of TiO_2 nanoparticles synthesized from Flame Stabilized by a Rotating Surface (FSRS) is predominantly anatase in fuel-lean flames, while rutile was dominant in fuel-rich flames. Existing phase equilibrium theories consider the surface area effect but are incapable of predicting the phase transition from oxygen-rich to oxygen-deficient flames. In this work, we made new measurements of TiO_2 nanoparticles over a range of equivalence ratio. The new measurements confirm the earlier findings. We propose an improved model for the surface energy contribution to the phase equilibrium that considers the role of surface bound oxygen and vacancies on surface energy. The model successfully explains the observations made here and in earlier publications. Specifically, model predictions are found to be in agreement with the experimental anatase and rutile compositions with respect to particle size and oxygen concentration. This result provides a promising phase equilibrium formulation for metal oxide nanoparticles that is more general than existing theories.
Keywords: Flame Synthesis, Titanium Dioxide, Nanoparticle, Crystal Phase

1. Introduction

Rutile and anatase are two common crystalline polymorphs of nano-scale titania (TiO_2) with wide-ranging differences in properties [1]. Bulk-phase anatase is known to be a metastable form of titania [2] but is used widely in nanostructured devices ranging from dye-sensitized solar cells [3], photoelectric chemical catalysis [4] to chemical sensors [5]. Studies of phase stability and transformation in TiO_2 extend from the classical work on bulk TiO_2 [6] to the somewhat more recent evaluations of nanoparticles [7-10]. The contribution of surface free energy is observed to play an important role in crystal-phase equilibrium especially for nano-size particles. By considering a surface contribution to Gibbs free energy, Zhang and Banfield [7, 8, 10] explained the rutile-to-anatase phase transition with impressive success; by considering surface energy (about 1 to 3 J/m^2) and surface stress of fully oxygenated TiO_2 surfaces, a thermodynamic phase diagram was constructed for TiO_2 nanoparticles in the size-temperature space using results of atomistic simulation of the surface energies [11]. In particular, the rutile-to-anatase transition diameter was predicted to be around 14 nm.

A previous flame synthesis study [12], however, indicates that the gas-phase composition may influence the phase equilibrium of TiO_2 particles. Anatase particles were observed for oxygen-rich growth conditions; while rutile was observed in oxygen deficient envionments with the size playing a minor role. The observation of stable rutile at diameters substantially smaller than 14 nm, the rutile-to-anatase crossover value predicted by Zhang and Banfield [8], suggests

that a more complete theory requires a consideration of the gas-particle surface equilibrium or the influence of oxygen desorption on nano TiO_2 crystal phase equilibrium.

In this work, the phase stability for nano-scale TiO_2 was assessed by treating the nature of the metal oxide surface/gas interface in a more generalized manner. In particular, the oxygen desorption/adsorption equilibrium was evaluated. Emphasis was placed on the high-temperature, chemically varying environment pertinent to flame-assisted chemical vapor deposition. The result is of interest to flame synthesis techniques, such as method of Flame Stabilized by a Rotating Surface (FSRS) [13, 14] have shown promising advantages for developing mesoporous metal-oxide thin-film applications [12].

2. Experiment

New FSRS synthesis experiments are carried out here with the purpose of further evaluating the sensitivity of nano-anatase and rutile phase stability with respect to the gas-phase envionment. Details of the FSRS technique have been described previously [12, 13, 15]. The synthesized TiO_2 nanoparticles were analyzed by X-ray diffraction (XRD). The weight fraction of anatase and rutile was determined using the method of Spurr and Meyers [16]. The correction factor for the relatively high intensity of the [101] peak of anatase as compared to the rutile [110] peak was taken to be 0.842, an average of values reported previously [7, 16]. Table 1 summarized the flame conditions considered, including six flames from a previous study [12] that are relevant to the current analysis. The gas-phase, equilibrium O_2 mole fraction was evaluated for each synthesis flame using the adiabatic assumption. In the FSRS post-flame region, particles nucleate, grow and undergo liquid-to-solid transformation as the gas jet approachs the chilled stagnation surface. Hence, the equilibrium O_2 concentration is indicative of the O_2 abundance in region where particles are synthesized. The measured particle size and phase composition is also summarized also in Table 1.

Table 1: Flame equivalence ratio (ϕ), equilibrium O_2 mole fraction ($x_{O_2,eq}$), and crystallite size and phase data of the TiO_2 particles synthesized.

flame	ϕ	T_{ad} (K)	$x_{O_2,eq}$	size (nm)	% anatase	% rutile	comments/ref
1a	0.52	2354	1.3×10^{-1}	11	91	9	[12]
1b	0.68	2551	8.5×10^{-2}	13	95	5	[12]
1c	0.83	2652	5.4×10^{-2}	13	71	29	[12]
2a	0.90	2651	3.7×10^{-2}	11	98	2	[12]
3a	1.13	2782	1.6×10^{-2}	8	20	80	[12]
4a	1.27	2797	9.3×10^{-3}	9	12	88	[12]
OR1	0.44	2385	1.8×10^{-1}	< 5	78	22	this work
OR2	0.46	2329	1.5×10^{-1}	11.3	93	7	this work
OR3	0.59	2667	1.5×10^{-1}	17.7	94	6	this work
OL1	1.19	2557	3.3×10^{-3}	< 5	30	70	this work
OL2	1.15	2560	4.4×10^{-3}	7.5	26	74	this work
OL3	1.33	2606	1.7×10^{-3}	12.1	29	71	this work

3. Theory

The size dependency of the TiO_2 particle crystal phase is explained in Zhang and Banfield [8] assuming a spherical particle shape. The Gibbs energy change of an anatase into rutile transformation is given as

$$\Delta G^{\circ}_{\text{anatase}\rightarrow\text{rutile}} = \Delta_f G^{\circ}_R(T) - \Delta_f G^{\circ}_A(T) + (2t+3)\frac{M}{r}\left(\frac{\gamma_R}{\rho_R} - \frac{\gamma_A}{\rho_A}\right), \quad (1)$$

where $\Delta_f G^{\circ}_R(T)$ and $\Delta_f G^{\circ}_A(T)$ are the Gibbs energy of formation of bulk-phase rutile and anatase, respectively, t is the ratio of surface stress to surface free energy, M is the molecular weight of TiO_2, and r is the particle radius. The surface free energy and density are denoted as γ and ρ with subscripts R and A indicating rutile and anatase. According to eq. (1), both bulk and surface properties play critical roles in nano-TiO_2 phase stability. The surface effect, namely the surface tension, increases as the particle size decreases, which is the primary cause for the size dependency of the TiO_2 crystal phase. Using the thermodynamic properties data from JANNAF [17] and the atomistic simulation result [11], Zhang and Banfield [8] found a critical diameter value of roughly 14 nm below which anatase becomes more stable than rutile – a prediction supported by the TiO_2 annealing experiment [7].

Oxygen thermodesorption has been shown to contribute to the chemical potential of bulk ruthenium surfaces [18]. It has been reported that under oxygen-lean or reducing conditions oxygen vacancy on bulk TiO_2 can be significant [6, 19]. Clearly, such vacancies would impact the surface energy. Futhermore, the gas-phase oxygen concentration impacts oxygen absorption and desorption on TiO_2 surfaces [2]: under oxygen deficient conditions, the reaction $2O^- \rightleftharpoons O_2(g) + 2s^-$ shifts to the right, leading to the formation of vacant sites s^-, which, in turn, influences the surface tension, perturbs the rutile-anatase phase equilibrium. Here, we evaluate this effect by estimating the equilibrium constant (K_p) of oxygen desorption from the TiO_2 surface.

The oxygen desorption enthalpy ΔH_r is reported to be 59 kcal/mol at 298K for anatase/rutile powder [20]. A measurement of the temperature dependency of oxygen desorption on the FSRS TiO_2 nanoparticles suggests that an activation energy of 50.4±0.4 kcal/mol for O_2 desorption at 773K [15]. Both values are substantiually smaller than that of oxygen desorption from bulk TiO_2. In the current work, we used 55 kcal/mol to model the enthalpy of oxygen desorption. The entropy and sensible enthalpy of $2O^-$ and $2s^-$ sites were assigned the values of solid-phase TiO_2 and Ti correspondingly. The surface density of vacancy was obtained from the equilibrium constant K_p and the gas-phase O_2 mole fraction x_{O_2} :

$$n_{s^-} == \frac{\sqrt{K_p / x_{O_2}}}{1 + \sqrt{K_p / x_{O_2}}} \quad (2)$$

For $x_{O_2} = 10^{-2}$ which correspond to an oxygen lean condition (see, Table 1), we find that n_{s^-} = 36% at 1500K.

To account for the surface oxygen desorption effect, we modify the second term in Eq. (1) to

$$\Delta G^{\circ}_{\text{anatase}\rightarrow\text{rutile}} = \Delta_f G^{\circ}_R(T) - \Delta_f G^{\circ}_A(T) + (2t+3)\frac{M}{r}\left(\frac{\gamma_{R/Ti}}{\rho_R} - \frac{\gamma_{A/Ti}}{\rho_A}\right), \quad (3)$$

where $\gamma_{R/Ti}$ and $\gamma_{A/Ti}$ are the surface free energies of rutile and anatase with surface oxygen partially desorbed. These free energies may be estimated by

$$\gamma_{R/Ti} = n_{s-}\gamma_{Ti} + \left(1-n_{s-}\right)\gamma_R$$
$$\gamma_{A/Ti} = n_{s-}\gamma_{Ti} + \left(1-n_{s-}\right)\gamma_A$$

In the above equations, γ_{Ti} is the surface free energy of pure titanium. The surface free energy γ_R and γ_A may be calculated from

$$\gamma(T) = \left[h(0\text{K}) + \int_0^T c(T)\,dT\right] - T\int_0^T \frac{c(T)}{T}\,dT\,, \tag{4}$$

where h(0K) is the surface free energy given by in Zhang and Banfield [8]: h_R(0K) = 1.93 J m^{-2} and h_A(0K) = 1.34 J m^{-2}. The surface specific heat $c(T)$ may be estimated by extrapolating from the low-temperature measurement [21] using the Debye theory [22]. We assumed here that the Debye temperature is 670K for TiO_2 [23], resulting in the surface specific heat values of 2.12, 2.30 and 2.33×10^{-4} (J m^{-2} K^{-1}) for T = 500, 1000 and 1500 K, respectively.

The surface free energy of titanium was estimated from its liquid phase $\gamma(T)\left(\text{J m}^{-2}\right) = 1.64 - 2.38\times10^{-4}\left[T(\text{K}) - 1043\right]$ [24]. The ratio of solid-to-liquid surface specific heat was taken to be 1.18 [25]. The thermal expansion was considered by treating the density ρ as a function of temperature. ρ decreases by ~5% as temperature increases from 300K to 2000K.

The Gibbs free energy of bulk rutile and anatase were taken from the JANAF table [17], which may be parameterized from 300 to 2000K as

$$\Delta_f G_R^\circ(T)\ \left(\text{J/mol}\right) = -9.46\times10^5 + 2.472\times10^2 T - 9.593T\ln T + 2.994\times10^{-3}T^2 - 3.472\times10^5 T^{-1} \tag{5}$$

$$\Delta_f G_A^\circ(T)\left(\text{J/mol}\right) = -9.41\times10^5 + 2.655\times10^2 T - 12.21T\ln T + 3.966\times10^{-3}T^2 - 2.603\times10^5 T^{-1} \tag{6}$$

Combining eqs. 2 and 3 and following Zhang and Banfield [8] by assuming t = 1, the phase equilibrium may be predicted as a function of particle radius r, gas-phase O_2 mole fraction x_{O_2}, and temperature T.

4. Reults and Discussion

As seen in Table 1, the flame equivalence ratio clearly impacts the rutile-to-anatase ratio. In particular, TiO_2 particles synthesized in oxygen-lean flames (3a, 4a, and OL1-3) are all dominated by rutile, despite the fact that the crystallite size is smaller than 14 nm, the rutile-to-anatase transition diameter originally proposed by Zhang and Banfield [8].

Figure 1 plots the $\Delta G^\circ_{\text{anatase}\to\text{rutile}}\left(T, r, x_{O_2}\right) = 0$ isolines at three representative temperatures. The $r - x_{O_2}$ region to the right of the line is anatase; and rutile is to the left of the line. Clearly, the formation of anatase is favored with high gas-phase O_2 concentrations and/or for small particle sizes, whereas rutile is favored in low-gas phase O_2 concentraitons and/or for large particles. The experimentally measured rutile-anatase partitions are also shown in the plot using the gas-phase equilibrium O_2 mole fraction calculated under the adiabatic condition. In the FSRS synthesis flames, the actual O_2 mole fraction that determines the phase equilibrium of the TiO_2 crystal phase is somewhat higher than the adiabatic equilibrium value because of

recombination at temperatures below the adiabatic flame temperture, but the difference is expected to be small. It can be seen that the 1800 K line divide the observed rutile-favored and anatase-favored conditions rather well. This result indicates the melting point of the TiO_2 nanoparticles prepreaed in FSRS to be around 1800 K. This temperature value is lower than the melting point of bulk TiO_2 at 2200K—an expected result due to the known dependency of metling point on particle size. The temperature value is also consistent with the result from a recent molecular dynamics simulation [26].

We now have a more complete picture of titania nanoparticle crystal phase equilibrium in the FSRS flames. Because the flame temperature is higher than the melting point of the particles, liquid droplets forms first behind the flame. As these droplets are transported away from the high-temperature region of the flame towards the cold stagnation surface, they solidifies. The crystal phase is determined largely by the gas-phase conditions during the solidification stage: the smaller particles in oxygen rich environment (lower left part of the phase diagram) turn to anatase, and the larger particles in oxygen lean environment turns to rutile.

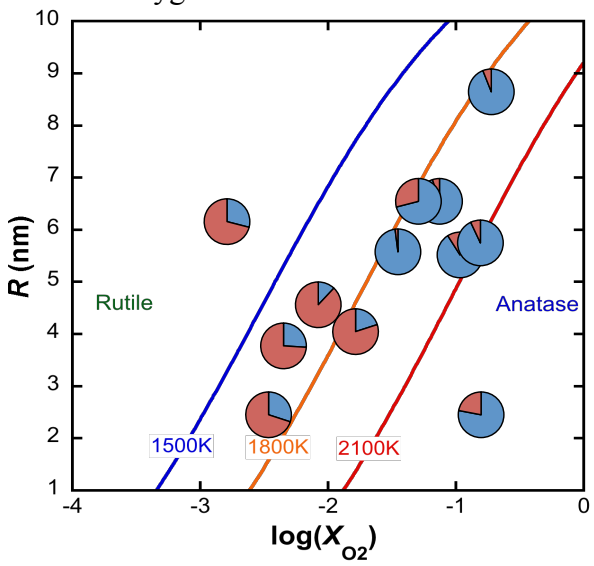

Figure 1. The $\Delta G^{\circ}_{\text{anatase}\rightarrow\text{rutile}}$ isolines in particle radius r vs. gas-phase O_2 mole fraction x_{O_2}. The blue fraction of the pie charts indicates measured anatase weight percentage, and the red fraction shows rutile weight percentage.

5. Conclusions

The analysis presented here illustrates the importance of oxygen thermodesorption to prediction of relative phase stability of nano TiO_2. Although the surface energy was not directly measured here, a clear dependency on the gas-phase O_2 concentration was demonstrated on the basis of a simple thermodynamic model. The analysis explained satisfactorily the unexpected observation of rutile dominance for particles produced in FSRS flames with sizes small than 14 nm.

6. References

[1] C. Di Valentin, G. Pacchioni, A. Selloni, Origin of the different photoactivity of N-doped anatase and rutile TiO_2, Phys. Rev. B 70 (8) (2004) article 085116.

[2] R. D. Shannon, J. A. Pask, Kinetics of the Anatase-Rutile Transformation, J. Am. Ceram. Soc. 48 (8) (1965) 391-398.

[3] S. Nikraz, H. Wang, Dye sensitized solar cells prepared by flames stabilized on a rotating surface, Proc. Combust. Inst. 34 (2) (2013) 2171-2178.

[4] P. Periyat, B. Naufal, S. G. Ullattil, A review on high temperature stable anatase TiO_2 photocatalysts, Mater. Sci. Forum 855 (2016) 78-93.
[5] J. Bai, B. Zhou, Titanium dioxide nanomaterials for sensor applications, Chem. Rev. 114 (19) (2014) 10131-10176.
[6] K. J. D. MacKenzie, The calcination of titania IV: The effect of reaction atmosphere and electric fields on the anatase-rutile transformation, Trans. & J. Br. Ceram. Soc. 74 (1975) 121-125.
[7] A. A. Gribb, J. F. Banfield, Particle size effects on transformation kinetics and phase stability in nanocrystalline TiO2, Am. Miner. 82 (7-8) (1997) 717-728.
[8] H. Zhang, J. F. Banfield, Thermodynamic analysis of phase stability of nanocrystalline titania, J Materi. Chem. 8 (9) (1998) 2073-2076.
[9] J. F. Banfield, H. Zhang, Nanoparticles in the environment, Rev. Miner. and Geochem. 44 (1) (2001) 1-58.
[10] H. Zhang, J. F. Banfield, Structural characteristics and mechanical and thermodynamic properties of nanocrystalline TiO_2, Chem, Rev. 114 (19) (2014) 9613-9644.
[11] P. M. Oliver, G. W. Watson, E. Toby Kelsey, S. C. Parker, Atomistic simulation of the surface structure of the TiO_2 polymorphs rutileand anatase, J. Mater. Chem. 7 (3) (1997) 563-568.
[12] S. Memarzadeh, E. D. Tolmachoff, D. J. Phares, H. Wang, Properties of nanocrystalline TiO2 synthesized in premixed flames stabilized on a rotating surface, Proc. Combus. Inst. 33 (2) (2011) 1917-1924.
[13] E. D. Tolmachoff, A. D. Abid, D. J. Phares, C. S. Campbell, H. Wang, Synthesis of nano-phase TiO_2 crystalline films over premixed stagnation flames, Proc. Combust. Inst. 32 (2) (2009) 1839-1845.
[14] H. Wang, Formation of nascent soot and other condensed-phase materials in flames, Proc. Combust. Inst. 33 (1) (2011) 41-67.
[15] E. Tolmachoff, S. Memarzadeh, H. Wang, Nanoporous Titania Gas Sensing Films Prepared in a Premixed Stagnation Flame, J. Phys. Chem. C 115 (44) (2011) 21620-21628.
[16] R. A. Spurr, H. Myers, Quantitative Analysis of Anatase-Rutile Mixtures with an X-Ray Diffractometer, Anal. Chem. 29 (5) (1957) 760-762.
[17] M. W. Chase, C. A. Davies, J. R. Downey, D. J. Frurip, R. A. McDonald, A. N. Syverud, J. Phys. Chem. Ref. Data 14 (1985) 1680-
[18] K. Reuter, M. Scheffler, Composition, structure, and stability of RuO_2 as a function of oxygen pressure, Phys. Rev. B 65 (3) (2001) article 035406.
[19] R. D. Shannon, Phase transformation studies in TiO_2 supporting different defect mechanisms in vacuum-reduced and hydrogen-reduced rutile, J.Appl. Phys.35 (11) (1964) 3414-3416.
[20] B. Halpern, J. E. Germain, Thermodesorption of oxygen from powdered transition metal oxide catalysts, J. Catal 37 (1) (1975) 44-56.
[21] J. Dugdale, J. Morrison, D. Patterson in: *The effect of particle size on the heat capacity of titanium dioxide*, Proceedings of the Royal Society of London A: Mathematical, Phys. & Eng. Sci., The Royal Society: 1954; pp 228-235.
[22] E. Gruneissen, Zur Theorie Der Spezifischen Waerme, Ann. Phys.(Leipzig) 39 (4) (1912) 789.
[23] H. J. McDonald, H. Seltz, The heat capacities of titanium dioxide from 68-298 °K. The thermodynamic properties of titanium dioxide, J. Am. Chem. Soc. 61 (9) (1939) 2405-2407.
[24] K. Zhou, H. Wang, J. Chang, B. Wei, Experimental study of surface tension, specific heat and thermal diffusivity of liquid and solid titanium, Chem. Phys. Lett. 639 (2015) 105-108.
[25] W. Tyson, W. Miller, Surface free energies of solid metals: Estimation from liquid surface tension measurements, Surf. Sci. 62 (1) (1977) 267-276.
[26] Y. Zhang, S. Li, W. Yan, S. D. Tse, Effect of size-dependent grain structures on the dynamics of nanoparticle coalescence, J. Appl. Phys. 111 (12) (2012) 124321.